Functional imaging of whole mouse embryonic development in utero

Jiejun Zhu[1], Dongming He[1], Mengzhu Sun[1,2], Hanming Zheng[1], Zihao Chen[1,2], Jin Yang[1], Chengqi Lin[3], Yun Stone Shi[1], Lei Sun[2*], Zhihai Qiu[1*]

[1]Guangdong Institute of Intelligence Science and Technology, Hengqin, Zhuhai, Guangdong 519031, PR China.

[2]Department of Biomedical Engineering, The Hong Kong Polytechnic University, Hung Hom, Hong Kong SAR 999077, PR China.

[3]School of Life Science and Technology, Key Laboratory of Developmental Genes and Human Disease, Southeast University, Nanjing 210096, PR China.

*Corresponding authors:

Zhihai Qiu, Ph.D

Room 2116, #6 building, International Innovation Center, Hengqin, Zhuhai

Guangdong Institute of Intelligence Science and Technology

PR China

Phone: (86)18084721235

Email: qiuzhihai@gdiist.cn

Lei Sun, Ph.D

Room ST409, Department of Biomedical Engineering,

The Hong Kong Polytechnic University,

Hong Kong SAR, PR China

Phone: (852) 2766 7663

Email: lei.sun@polyu.edu.hk

Abstract

Investigation into early embryonic functions, e.g. brain activity, have long been constrained due to the technical challenges involved. Functional ultrasound (fUS) has emerged as a breakthrough modality for real-time monitoring of brain activity, offering considerable potential as a tool for studying functional embryonic development. In the present study, fUS was leveraged to monitor the functions of developing mice from embryonic days E8.5 to E18.5, revealing its ability to capture whole-embryo activity with exceptional spatial and temporal resolutions. The data revealed a high correlation between cardiac function and body size, underscoring the pivotal role of cardiac function in embryonic growth. Moreover, brain activity across the gestational period was successfully captured, providing valuable information about brain activity during embryonic/fetal development. Thus, our study offers novel insights into embryonic functional development, laying the foundation for embryonic fUS imaging in both scientific research and clinical contexts.

Introduction

Much of the current understanding of mammalian embryonic development has been gained from studying anatomical dissections of animals and organoids (*1-3*), which have revealed critical time-points for embryogenesis, organogenesis, and their corresponding gene factors. Metabolic states, similarly, have been found to regulate vascular and neural development at different embryonic stages (*4-6*). Modern molecular biological methods such as single-cell RNA sequencing and spatial transcriptomics have further enriched our understanding, uncovering the neuronal-type hierarchy and the potential vulnerabilities for neurodevelopmental disorders, including autism (*7*). However, these studies are limited by discontinuous time observations and lack real-time monitoring of changes.

To address this problem, several kinds of functional imaging technologies have been developed to gain deeper insight into embryonic/fetal development. Optical methods, including two-photon microscopy and light-sheet microscopy, have proven invaluable for imaging *C. elegans*, *Drosophila* and zebrafish (*8*), providing detailed insights into whole-embryo cellular-level development. However, when it comes to applying optical methods to mammalian embryos, the ability to gain a comprehensive view of the whole embryo becomes curtailed (*9*). Recently, a study utilized photoacoustic microscopy to capture both the structure and function of the heart during gestational days (GDs) 14.5–17.5 (*10*), while another study using the same method focused on capturing placental function under both normal and pathological conditions (*11*). However, these methods are limited in the transparency they offer and, thus, do not permit whole-embryo observation. Without a holistic perspective, we cannot fully grasp how different organs function, interact, and coordinate with each other during development, ultimately culminating in the successful emergence of a new life. Magnetic resonance imaging (MRI) provides sufficient coverage of the entire fetus (*12*) but it primarily evaluates only structural features. A modified approach, functional magnetic resonance imaging (fMRI), is capable of exploring the

functional characteristics of the brain (*13-15*), but it has limited application in the fetal context having poor resolution and motion artifacts (*16, 17*). Nevertheless, the fundamental principle of fMRI remains sound - it assesses hemodynamic changes that mirror brain function, operating under the assumption that the heightened energy demand during brain activity necessitates circulatory support (*13*).

Building upon this principle, functional ultrasound (fUS) imaging was recently introduced as a modality for real-time monitoring brain activity in the rodent, and macaque (*18-20*). Given the rapid growth of the embryo, which necessitates robust blood flow to meet its energy demands, this method is particularly apt for evaluating embryonic function. fUS offers a distinctive blend of attributes, including expansive spatial coverage (up to 10 cm), high spatiotemporal resolution (down to 100 μm and up to 10 ms), and ample sensitivity (detecting relative hemodynamic changes of as little as 2% without the need for averaging across multiple trials) (*19-21*). Thus, fUS as a modality offers the potential for effective, comprehensive monitoring of fetal hemodynamic activity with high spatiotemporal resolution without being hampered by typical anatomical limitations.

In this study, we aimed to establish fUS as a potential tool to monitor functional activities of developing mouse embryos. Our data revealed that fUS effectively images the entire mouse embryo, offering exceptional sensitivity and spatiotemporal resolution from E8.5 to E18.5. By employing this method, we uncovered a noteworthy correlation between cardiac function and body size throughout the gestational period. By deconvoluting brain fUS signals from those of the heart, we were able to capture independent brain activities across the gestational period, with an increase of delta rhythm observed from E13.5 and a slightly decrease in E18.5. Taken together, our study provides novel insights into embryonic functional development. With the existent widespread use of fetal ultrasound in clinical settings, our findings lay a foundation for advancing fetal examination techniques and possible early detection of disorders or conditions.

Results

Functional Ultrasound Imaging Captures Embryonic Functioning with Exceptional Spatial and Temporal Resolution Across Depth

Functional ultrasound (fUS) imaging utilizes plane waves of ultrasound to provide accurate, high-resolution images of mouse embryos *in vivo* in a fully non-invasive manner (Movie S1). To mimic *in utero* ultrasound in the clinic (*22, 23*), we performed the fUS in a minimally-invasive way in the following experiment (Fig. 1). Performing fUS by acquiring 25 compound images at 500 Hz, each one from 7 planar illuminations tilted from −6° to 6° by a 15-MHz ultrasound probe, we were able to image the whole mouse embryo (12.8 * 10 mm) in a very short acquisition time (50 ms). In this way, a time-resolved readout of the blood volume variation within each voxel in a whole embryo could be recorded.

Compared to traditional B-mode ultrasound imaging, fUS images, projected by 2-second fUS signals (consisting of 1000 compound images), provide significantly richer information about the embryonic circulation system (Fig. 2A-D). Moreover, employing stepped scanning enables clear visualization of the sagittal, coronal, and horizontal planes of the embryonic circulation system, allowing for detailed observation of functions in regions such as the placenta, spinal cord, brain vascular networks, and more (Movies S2, S3, and S4).

Importantly, fUS can capture embryonic circulation as early as E8.5, when the heart tube is first formed (see Movie S5, Fig. 2E), supported by the pattern of CD31 vascular staining (Fig. 2F). Analysis of the intensity distribution of fUS signals in the dorsal aorta revealed a full-width at half maximum (FWHM) approximately 4.7 times greater than that of the corresponding immunofluorescence (IF) signal (375 μm vs. 78.8 μm) (Fig. 2G). Similarly, fUS enabled the capture of vessels in the mouse spinal cord and brain, with a FWHM of 277.05±15.72 (Mean ± SEM, Fig. 2H) and 242.87 ± 27.07 (Mean ± SEM, Fig. 2J) respectively. These findings underscore the exceptional spatial resolution of fUS, capable of detecting heart and brain function in embryos.

Cardiac Functions Display Varying Distinctive Patterns During Embryonic Development

Utilizing fUS, we were able to visualize cardiac functions with a heartbeat cycle of approximately 0.6 seconds at E16.5 (Fig. 3A). The full width at half maximum (FWHM) of the heart fUS signal was measured at 0.15 seconds (Fig. 3B). To assess the sensitivity of fUS in embryonic studies, we conducted further tests on cardiac functions in embryos at early stages of heart development. Remarkably, at E8.5 when the heart is still in the form of a heart tube, fUS signals for each individual heartbeat could be accurately captured (FWHM = 0.15 s) (Fig. 3C-D). This level of precision provides ample resolution for investigating the circulatory system throughout the entire gastrulation period.

Building on this finding, we further investigated heart activity from E8.5 to E18.5 (Fig. 3E-F). fUS imaging was acquired by positioning the ultrasonic transducer over the uterine sac-encased embryos, which were extracted through a small vertical abdominal incision. The transducer was adjusted to locate the embryos and the beating heart, and to orient the sagittal plane of the embryo.

After identifying the heart at its highest intensity plane, fUS imaging of the entire embryo was conducted for a continuous period of 600 seconds. The functions of different embryos were recorded independently, revealing repeated cycles of heart functions. Importantly, each cycle was clearly observed with a trace of blood flow from the heart to distal regions including the brain and placenta. Given this repetitive nature and the observable blood flow trace (Movie S5-S6), it is conceivable that each cycle represents one complete heartbeat. We could detect an increase in heart rate as the embryo developed (Fig. 3G), consistent with prior research (*24*). Furthermore, upon analyzing the cardiac function patterns, we identified distinct classifications: 1-peak, 2-peak, 3-peak or 4-6-peak patterns (Fig. 3H-I), which exhibited notable variations during embryonic development. During the early stages (E8.5-E11.5), we observed a dominant 4-6 peak pattern which may indicate irregular and uncoordinated contractions of the immature heart and disturbed blood flow during chamber

formation (*25*). Subsequent decrease of this pattern likely reflects the progress of heart development. The steady increase of the 2-peak pattern indicates more coordinated blood flow in and out of the heart. The progressive increase in the 3-peak pattern may indicate ventricular blood flow induced by negative pressure in the atrium, positive pressure in the atrium and ventricular pumping, signaling the gradual maturation of heart chambers and valves (*25, 26*). However, it remains unclear why there is a drop of the 3-peak pattern at E16.5 and E18.5 (Fig. 3J-K). Aggregating all heartbeat patterns, we consistently observed the prevalence of the 2-peak pattern across the entire gestation, accompanied by a reduction in the duration of each heartbeat cycle (Fig. 3L). In this manner, fUS revealed identifiable functional differences of the heart at different stages of fetal development.

Intensity of Cardiac fUS Signal Couples with Body Size in Embryonic Mice

In our study, we observed a highly efficient blood supply system wherein each heartbeat occurs only after blood flow has ceased in the distal regions (movie S5-S6; Fig. 4D). This suggests a developmental relationship between cardiac function and body size. fUS signals were monitored and recorded from embryonic cardiac function (Fig. 4A) alongside measurements of embryonic size (Fig. 4B) from E9.5 to E18.5. Both parameters exhibited a consistent increase throughout embryonic development. Furthermore, in line with our hypothesis, we found a high degree of correlation between cardiac fUS signals and body size ($R^2=0.751$; Fig. 4C).

Embryonic Brain Activity Can Be Monitored Through Functional Ultrasound Imaging Independent of Heart Pulses

By analyzing features of major cerebral arteries, such as the anterior cerebral artery and posterior cerebral artery, alongside B-mode features, we successfully segmented the brain into the forebrain, midbrain, and hindbrain regions (Fig. 5A). Remarkably, the fUS signals of both the heart and brain could be simultaneously studied within a single embryo (Fig. 5A-B). In our study, we found a strong influence

of heart activity on the brain, where the initiation of each heartbeat cycle coincided with brain signals (movies S7, Fig. 5C). Further examination of these signals showed that brain responses followed heartbeats within 0 to 200 ms, as indicated by the optimal lag for achieving the highest correlation between heart and brain signals (Fig. 5D-E). While previous studies suggest that fUS signals reflect neuronal activity in the adult mouse brain (*27*), the pronounced correlation between heart and brain signals in developing mouse embryos indicates an overwhelming influence of cardiac signals.

Recently, a study revealed the heart's impact on adult mouse brain activity through blood pulsations, affecting mitral cells in the olfactory bulb (*28*). To mitigate artifactual of fUS signals induced by blood flow pulsation, we conducted a deconvolution analysis. Post-deconvolution, clear brain signals were discernible across all brain regions, including the forebrain, midbrain, and hindbrain (Fig. 5F). Moreover, cross-correlation analysis of different brain regions, such as forebrain to midbrain, forebrain to hindbrain, and midbrain to hindbrain, revealed similar correlation patterns over the gestational period, reaching their lowest levels at E13.5 and highest at E16.5 (Fig. 5G). Additionally, we categorized brain signals into three aspects: slow waves exhibiting a delta rhythm below 4 Hz, rapid waves within the theta range of 6 to 10 Hz, and other epochs with an even rhythm distribution (Fig. 5H). Analyzing these three patterns, we observed temporal changes in brain activity (Fig. 5I). Fluctuations were found in these patterns throughout the entire developmental period, with an increase of delta rhythm at E13.5 (Fig. 5J). Intriguingly, the timing of these changes correlates with the metabolic shifts in the brain during this period (*4-6*). Capable of monitoring the whole embryonic functional activity during development, fUS could serve as an interface between embryo in utero and the external world. To demonstrate this concept, we encode the brain activity of three different brain regions into three audible sound frequencies (Mm. 1). It is easy for a human brain to decode the nature of brain activity from the audible sound as a read of embryonic brain activities. This could provide a way for the mother to hear and monitor the fetal brain state.

Discussion

Fetal ultrasound stands as the primary technique for prenatal examinations in clinics, offering detailed structural information about the fetus and its cardiac function throughout the gestational period. Our proof-of-concept study showcases functional ultrasound (fUS) imaging, a method that harnesses the same physics used in existing fetal ultrasound while offering novel functional insights. This represents a significant advancement in embryonic imaging which could revolutionize fetal examination in the clinical realm.

By directly observing whole-embryo blood flow from E8.5 to E18.5 (Movie S5-S6), one can easily appreciate the importance of blood perfusion during development. It has been hypothesized that cardiac functions play a pivotal role in embryonic growth (*29*). Intriguingly, we found a significant correlation between cardiac function and body size throughout the gestational period supporting this well-known hypothesis. Assuming that whole-embryo blood circulation is a highly efficient system, it remains unclear whether the heart's pumping ability exerts an influence on body development or vice versa. On the other hand, the strong influence of blood flow pulsation observed on the brain may modulate neurodevelopment directly. It has been shown that blood pressure pulsations modulate mechanosensitive olfactory bulb neurons in mice (*28*). This suggests that cardiac function could modulate neurodevelopment in CNS, given the fact that various cells express high levels of mechanosensitive ion channels in the developmental stages (*30, 31*). Further study of this important developmental relationship between discrete fetal regions could be well-served by the ease and efficiency of fUS monitoring.

Significantly, our utilization of fUS with deconvolution of heartbeat signals facilitated the monitoring of brain activity throughout the gestational period, revealing a delta rhythm patterns of brain activity emerging at E13.5 and slightly decreasing at E18.5. These time points coincide with the increasing vascularization in the ventricular zone (VZ), the transition of cortical neural progenitor cell (NPCs) to neurogenic divisions and the NPCs to aerobic metabolism at E13.5, and a fraction of

RGPs progresses into the gliogenic phase at E16.5 (*4-6*). The delta rhythm pattern in embryonic mouse brains may thus indicate a high level of these processes, serving as a criterion to evaluate normal brain development during gestation.

Fetal ultrasound measurements of eye movement, heartbeat, and breathing are the only way to predict fetal brain activity to date (*32*). Our fUS method opens new avenues of research into embryonic brain activity, offering valuable insights into early brain function and development. The delta rhythm corresponds to the NREM sleep pattern identified by EEG in grown animals (*33*). However, the timing of its changes in utero is not known with certainty as fetuses are embedded *in utero*, and therefore not accessible for traditional EEG recording. Consistent with our data, the data from premature infants and adult predict that there should be an increase in late embryonic stage (*34*). While further investigations are warranted to explore the nature of this pattern and the potential correlation between brain development and sleep origin, our discovery here unveils novel pathways for scrutinizing early brain development and activity, particularly in the enigmatic realm of fetal consciousness exploration.

In our study, functional ultrasound (fUS) imaging demonstrated its capability to capture the dynamic functions of mouse embryos in utero. This opens the door for early detection of fetal diseases, disorders, or other conditions. We envision that the dynamic nature of functional changes captured by fUS may pave the way for embryo-computer interfaces combined with non-invasive intervention methods such as ultrasound neuromodulation. This will enhance our understanding of embryonic development and developmental disorders, perhaps allowing for earlier intervention and remediation.

Conclusion

In this study, we discovered that fUS effectively captures the functioning of the whole mouse embryo throughout the gestation period with exceptional sensitivity and spatiotemporal resolution. Specifically, we found a high correlation between cardiac function and body size, underscoring the pivotal role of cardiac function in embryonic

growth. Independently of signals from heart pulsations, we were able to capture intricate and specific patterns of brain activity. The successful capture of brain activity opens new avenues for research into embryonic brain activity, providing valuable insights into patterns of early brain development. In summary, our study offers novel insights into embryonic functional development, paving the way for further in utero studies of fetal development.

Reference and Notes

1. T. W. Sadler, *Langman's medical embryology*. (Lippincott Williams & Wilkins, 2022).
2. L. Wolpert, C. Tickle, A. M. Arias, *Principles of development*. (Oxford University Press, USA, 2015).
3. S. C. van den Brink *et al.*, Single-cell and spatial transcriptomics reveal somitogenesis in gastruloids. *Nature* **582**, 405-409 (2020).
4. R. Boon, G. G. Silveira, R. Mostoslavsky, Nuclear metabolism and the regulation of the epigenome. *Nature Metabolism* **2**, 1190-1203 (2020).
5. X. Dong *et al.*, Metabolic lactate production coordinates vasculature development and progenitor behavior in the developing mouse neocortex. *Nat Neurosci* **25**, 865-875 (2022).
6. D. Z. Doyle, K. Y. Kwan, Neurogenic-angiogenic synchrony via lactate. *Nat Neurosci* **25**, 839-840 (2022).
7. T. J. Nowakowski *et al.*, Spatiotemporal gene expression trajectories reveal developmental hierarchies of the human cortex. *Science* **358**, 1318-1323 (2017).
8. C. Singleman, N. G. Holtzman, Analysis of postembryonic heart development and maturation in the zebrafish, Danio rerio. *Dev Dyn* **241**, 1993-2004 (2012).
9. Q. Huang *et al.*, Intravital imaging of mouse embryos. *Science* **368**, 181-186 (2020).
10. M. Hatami *et al.*, Noninvasive Tracking of Embryonic Cardiac Dynamics and Development with Volumetric Optoacoustic Spectroscopy. *Adv Sci (Weinh)*, e2400089 (2024).
11. X. Zhu *et al.*, Longitudinal intravital imaging of mouse placenta. *Science Advances* **10**, eadk1278 (2024).
12. S. N. Saleem, Fetal MRI: An approach to practice: A review. *J Adv Res* **5**, 507-523 (2014).
13. S. Ogawa, T.-M. Lee, A. R. Kay, D. W. Tank, Brain magnetic resonance imaging with contrast dependent on blood oxygenation. *proceedings of the National Academy of Sciences* **87**, 9868-9872 (1990).
14. R. B. Buxton, *Introduction to functional magnetic resonance imaging: principles and techniques*. (Cambridge university press, 2009).
15. K. Rubia, Functional brain imaging across development. *Eur Child Adolesc Psychiatry* **22**, 719-731 (2013).
16. Q. Yu, L. Leatherbury, X. Tian, C. W. Lo, Cardiovascular assessment of fetal mice by in utero echocardiography. *Ultrasound Med Biol* **34**, 741-752 (2008).
17. T. Deffieux, C. Demene, M. Pernot, M. Tanter, Functional ultrasound neuroimaging: a review of the preclinical and clinical state of the art. *Curr Opin Neurobiol* **50**, 128-135 (2018).

18. E. Mace *et al.*, Functional ultrasound imaging of the brain: theory and basic principles. *IEEE Trans Ultrason Ferroelectr Freq Control* **60**, 492-506 (2013).
19. A. Dizeux *et al.*, Functional ultrasound imaging of the brain reveals propagation of task-related brain activity in behaving primates. *Nat Commun* **10**, 1400 (2019).
20. S. L. Norman *et al.*, Single-trial decoding of movement intentions using functional ultrasound neuroimaging. *Neuron* **109**, 1554-1566 e1554 (2021).
21. C. Demene *et al.*, Functional ultrasound imaging of brain activity in human newborns. *Science translational medicine* **9**, eaah6756 (2017).
22. T. Stampalija, G. M. Gyte, Z. Alfirevic, Utero‐placental Doppler ultrasound for improving pregnancy outcome. *Cochrane Database of Systematic Reviews*, (2010).
23. R. Hering-Hanit, R. Achiron, S. Lipitz, A. Achiron, Asymmetry of fetal cerebral hemispheres: in utero ultrasound study. *Archives of Disease in Childhood-Fetal and Neonatal Edition* **85**, F194-F196 (2001).
24. R. C. V. Tyser, S. Srinivas, The First Heartbeat-Origin of Cardiac Contractile Activity. *Cold Spring Harb Perspect Biol* **12**, (2020).
25. L. Andrés-Delgado, N. Mercader, Interplay between cardiac function and heart development. *Biochimica et Biophysica Acta (BBA) - Molecular Cell Research* **1863**, 1707-1716 (2016).
26. Y.-H. Gui, K. K. Linask, P. Khowsathit, J. C. Huhta, Doppler Echocardiography of Normal and Abnormal Embryonic Mouse Heart. *Pediatric Research* **40**, 633-642 (1996).
27. A. O. Nunez-Elizalde *et al.*, Neural correlates of blood flow measured by ultrasound. *Neuron* **110**, 1631-1640 e1634 (2022).
28. L. Jammal Salameh, S. H. Bitzenhofer, I. L. Hanganu-Opatz, M. Dutschmann, V. Egger, Blood pressure pulsations modulate central neuronal activity via mechanosensitive ion channels. *Science* **383**, eadk8511 (2024).
29. H. P. Gutgesell, C. M. Rembold, Growth of the human heart relative to body surface area. *The American journal of cardiology* **65**, 662-668 (1990).
30. S. G. Lechner, H. Frenzel, R. Wang, G. R. Lewin, Developmental waves of mechanosensitivity acquisition in sensory neuron subtypes during embryonic development. *The EMBO journal* **28**, 1479-1491 (2009).
31. D. E. Koser *et al.*, Mechanosensing is critical for axon growth in the developing brain. *Nature neuroscience* **19**, 1592-1598 (2016).
32. J. C. Birnholz, The development of human fetal eye movement patterns. *Science* **213**, 679-681 (1981).
33. Y. Oishi *et al.*, Polygraphic Recording Procedure for Measuring Sleep in Mice. *J Vis Exp*, e53678 (2016).
34. J. A. Hobson, REM sleep and dreaming: towards a theory of protoconsciousness. *Nat Rev Neurosci* **10**, 803-813 (2009).
35. C. Brunner *et al.*, Whole-brain functional ultrasound imaging in awake head-fixed mice. *Nat Protoc* **16**, 3547-3571 (2021).

Acknowledgments:

Funding: This work is supported in part by the National Natural Science Foundation of China (32371151), Guangdong High Level Innovation Research Institute (2021B0909050004), the Hong Kong Research Grants Council Collaborative Research Fund (C5053-22GF), General Research Fund (15224323 and 15104520), Hong Kong Innovation Technology Fund (MHP/014/19), internal funding from the Hong Kong Polytechnic University (G-SACD and 1-CDJM).

Author contributions: Conceptualization: ZHQ, JJZ, Methodology: JJZ, ZHC, DMH, MZS, HMZ. **Funding acquisition:** ZHQ, LS, CQL, JY. **Project administration:** ZHQ, JJZ. **Supervision:** ZHQ. **Competing interests**: The authors declare that they have no competing interests. **Data and materials availability:** All data are available in the main text or the supplementary materials.

Supplementary Materials

Materials and Methods
Movies S1 and S7
Mm.1

Materials and Methods

Mice

C57BL/6J mice were obtained from Bestest (Zhuhai, China) and mated overnight. The morning that plugs were detected was considered as embryonic day (E) 0.5. Mice were housed with a regular dark–light cycle and fed a standard diet and water *ad libitum*. All mouse procedures were performed following the guidelines of the Committee of Use of Laboratory Animals, Guangdong Institute of Intelligence Science and Technology, China.

Functional ultrasound imaging of embryonic heart and brain

Pregnant mice from E8.5 to E18.5 were used of the experiment. Anesthetized pregnant mice (Zoletil-50 50mg/kg and Xylazine 2.6mg/kg, ip injection) were placed supine on a constant temperature insulation mat maintained at 37°C. Fur was removed from the region of the belly overlying the uterus, and a small vertical incision was made into the abdomen. Through this incision, embryos, still encased within their uterine sac, were extracted, and placed outside the mouse's abdominal cavity. To ensure that the heart and brain could be imaged on the same plane, the embryos were positioned with their dorsal sides facing up or down, which allowed for access to the sagittal plane with a probe. Embryos were carefully covered with bubble-free ultrasound gel and subsequently imaged. The basic imaging protocol was derived from the established open-source method, miniScan(*35*). Imaging was performed using an ultrasound scanner (Verasonics, Vantage 256) in conjunction with a linear ultrasound transducer (Verasonics, L22-14Vx), achieving a spatial resolution approximately 100 μm/pixel. To enhance real-time computing capabilities and increase temporal resolution, a professional-grade graphical computing card (Nvidia Quadro RTX4000) was integrated, enabling a recording frequency of 20 Hz.

Analysis

fUS data were analyzed using MATLAB by selecting regions of interest to extract blood flow signals from the frontal, central and posterior brain regions as well as the heart. Thresholds were set for cardiac cycle width and peak amplitude to automatically identify the number of heartbeats within the heart blood flow signal. Peak classification was implemented based on the number of peaks per cycle to statistically analyze the proportions of 1-, 2-, 3-, and 4-6-peaked heart blood flow waveforms at different gestational ages.

Correlations between brain blood flow signals and between brain and cardiac blood flow signals were analyzed using MATLAB. A 0.3 Hz high-pass filter was applied to extract purer brain blood flow signals by removing low frequency noise. Deconvolution filtering was utilized to remove interfering cardiac blood flow and harmonic components mixed within the brain signals.

Autoregressive power spectral estimation was performed over 10 s intervals on extracted frontal, central and posterior brain blood flow waveforms. Functional states for each 10 s interval were classified into three categories by comparing energy levels between 0.5-5 Hz and 6-10 Hz: focused in low frequencies (0.5-5 Hz), high frequencies (6-10 Hz), or without clear frequency features. These were respectively indicated by blue, purple and yellow stripes on the time-frequency map for long-term observation of changes in brain functional activity states. The proportions of the three functional states at different gestational ages were also statistically analyzed. Furthermore, the brain blood signals were converted into sound sequences according to the spectral distribution within every 10 seconds, in order to encode the time structure of the brain activity into sound sequences.

Immunohistochemical Fluorescent Staining

For E8.5 embryos, following dissection from the uteri of pregnant mice, postfixation was performed at room temperature for 4 hours using 4% PFA. Following post-fixation, specimens were rinsed with PBS. Embryos were then incubated overnight at 4°C in a blocking solution containing 10% normal goat serum, 1% bovine serum albumin, and 0.3% Triton X-100. After blocking, embryos were incubated with CD31 antibody (1:50; Cat. No. ab7388, Abcam) for two nights at 4°C and then with Alexa Fluor 555-conjugated Donkey anti-rat secondary antibody (1:50; Cat. No. A11077, Invitrogen). Light-sheet images were captured by LiTone XL Light-sheet Microscope (Light Innovation Technology Limited) with a 10X objective (N.A.= 0.6). Further image processing was performed by LitScan 3.2.0 (Light Innovation Technology Limited).

Figures

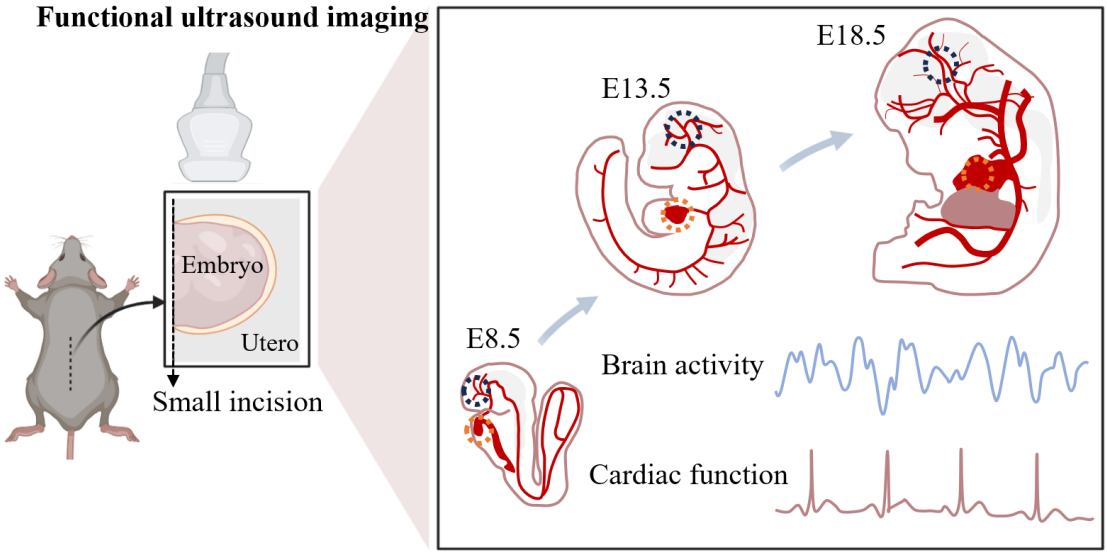

Fig. 1: Schematic representation of embryonic functional ultrasound imaging throughout the gestational period

Schematic representation of a pregnant mouse undergoing functional ultrasound imaging (left). An embryo, still inside its uterus, was extracted through a small incision in the pregnant mouse's abdomen (middle). Embryos ranging from E8.5 to E18.5 were imaged, and their cardiac function and brain activity were analyzed (right).

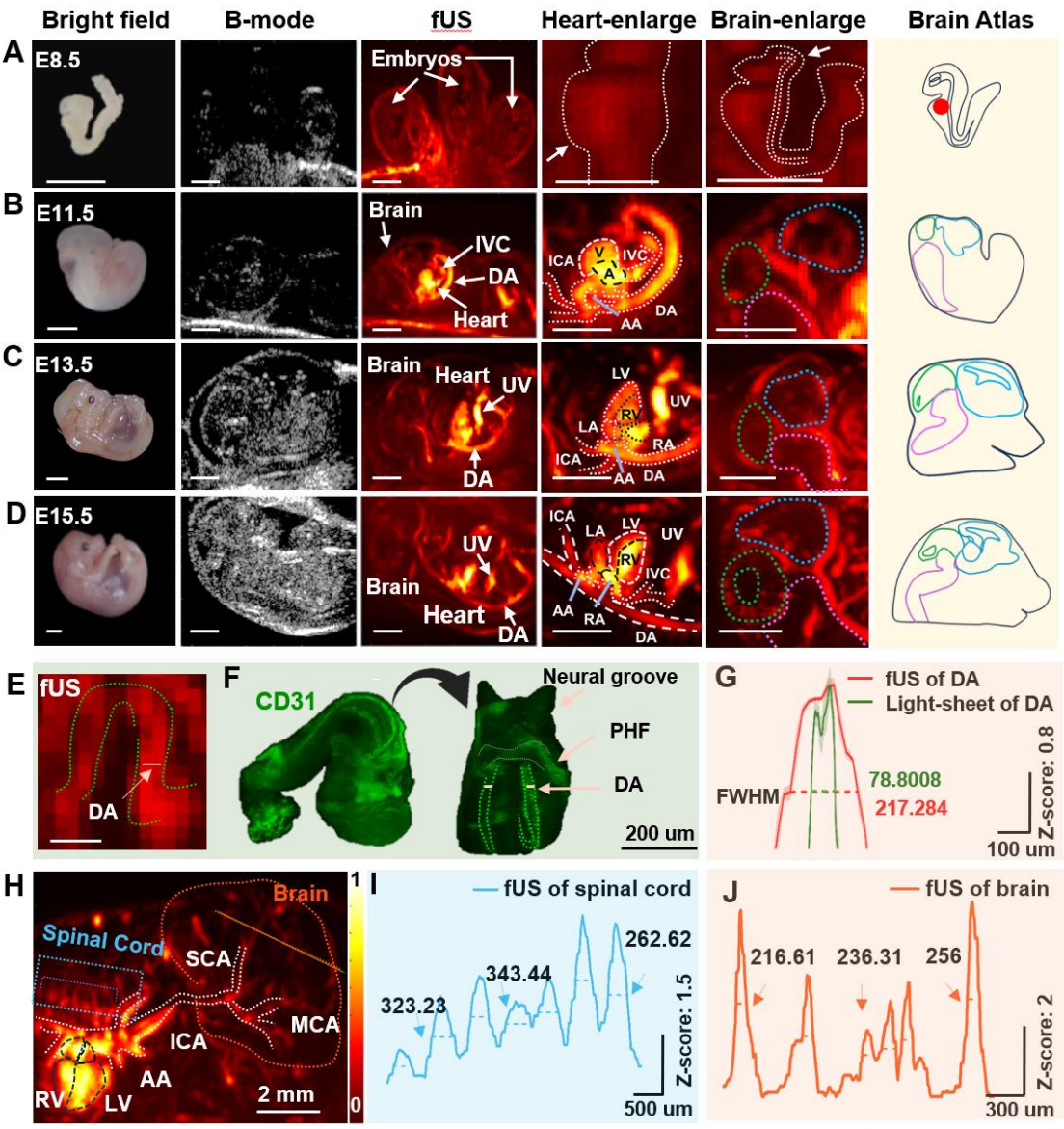

Fig. 2: Functional ultrasound imaging captures whole embryonic functions with exceptional sensitivity and spatiotemporal resolution

A) Representative images of E8.5 mouse embryos under (from left to right) bright field, B-mode ultrasound, fUS, heart fUS enlarged, brain fUS enlarged, and the corresponding brain atlas images. Scale bars: 2mm.

B) Representative images of E11.5 mouse embryos. Scale bars: 2mm.

C) Representative images of E13.5 mouse embryos. Scale bars: 2mm.

D) Representative images of E15.5 mouse embryos. Scale bars: 2mm.

E) Representative imaging frame of fUS data obtained from an E8.5 embryo within a heartbeat cycle. Green dotted lines delineate the dorsal aorta (DA). White dotted line indicates

the DA region (DA diameter) targeted for further analysis. Scale bar: 1mm.

F) Light-sheet imaging of an E8.5 embryo stained with CD31 (an endothelial marker of blood vessels). Green dotted lines delineate the embryonic DA. White dotted lines indicate the DA region (DA diameter) targeted for further analysis.

G) Signal intensity along the vertical axis of the dorsal aorta of the E8.5 embryo presented in E and F panel. The full width at half maximum (FWHM) of fUS is 375 μm, and the FWHM of light-sheet imaging is 78.8 μm.

H) Representative imaging frame of fUS data obtained from an E16.5 embryo. White lines dotted lines indicate major organs and vessels. Blue dotted line and orange dotted line indicate the spinal cord and a randomly drawn line across the brain vessels for subsequent analysis.

I) Distribution of fUS signal intensity of spinal cord blood flow along the blue lines in panel H The FWHM values are 242.42, 323.23, 242.42, 343.44, 282.82, 242.43 and 262.62 μm.

J) Distribution of fUS signal intensity of brain blood flow along the origin lines in panel H. The FWHM values are 216.61, 216.61, 236.31, 295.39, 236.3, and 256 μm.

Abbreviations in Fig. 2: A, atrium; AA, aortic arch; DA, dorsal aorta; ICA, internal carotid artery; IVC, inferior vena cava; LA, left atrium; LV, left ventricle; MCA, middle cerebral artery; PHF, primary heart field RA, right atrium; RV, right ventricle; SCA, superior cerebellar artery; UV, umbilical vein; V, ventricle.

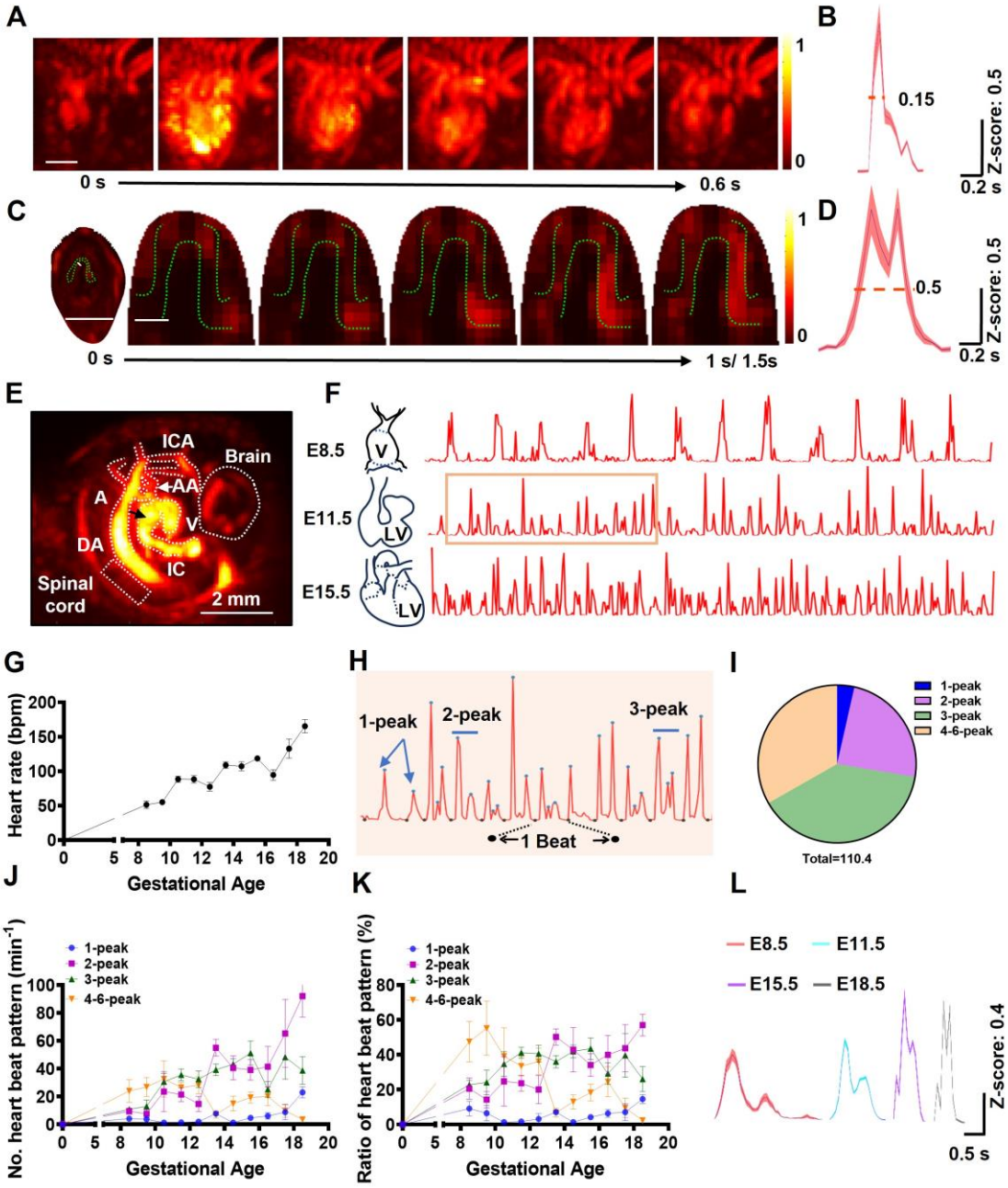

Fig. 3: Cardiac Functions Display Varying Distinctive Patterns With Embryonic Development

A) Representative image sequence of heart fUS signals within a heartbeat cycle obtained from an E16.5 embryo. Scale bar: 1mm.

B) Averaged fUS signal of the heart within a heartbeat cycle. The FWHM is 0.15 seconds.

C) Representative image sequence of heart fUS signals within a heartbeat cycle obtained from an E8.5 embryo. Scale bar: 2mm & 1mm.

D) Average fUS signal (blood flow) of the heart within a heartbeat circle. The FWHM is 0.5

seconds.

E) Representative fUS imaging frame from an E11.5 embryo. White dotted lines indicate major organs and vessels.

F) Morphological exemplars of the embryonic heart (left) and their corresponding fUS signals (right) in E8.5, E11.5, and E15.5 embryos (top to bottom).

G) Summary of embryonic heartbeats ranging from E8.5 to E18.5 (n=3-4 in each group). Data presented as Mean ± SEM.

H) Enlarged E11.5 embryonic heart fUS signals, repeated cycles of bursts can be clearly observed. Classifications of 1-peak, 2-peak, and 3-peak of cardiac function patterns is indicated.

I) Exemplar of the 1-peak, 2-peak, 3-peak and 4-6-peak cardiac function patterns distribution within an E15.5 mouse.

J) Summary of the number of 1-peak, 2-peak, 3-peak and 4-6-peak of cardiac function patterns ranging from E8.5 to E18.5 (n=3-4 in each group). Data presented as Mean ± SEM.

K) Summary of the ratio of 1-peak, 2-peak, 3-peak and 4-6-peak of cardiac function patterns ranging from E8.5 to E18.5 (n=3-4 in each group). Data presented as Mean ± SEM.

L) Exemplars of fUS signals of embryonic cardiac function pattern during one heartbeat period from E8.5, E11.5, E15.5 and E18.5 embryos (red, indigo, purple and grey).

Abbreviations in Fig. 3: DA, dorsal aorta; V, ventricle; A, atrium; ICA, internal carotid artery; AA, aortic arch; IC, inferior cava.

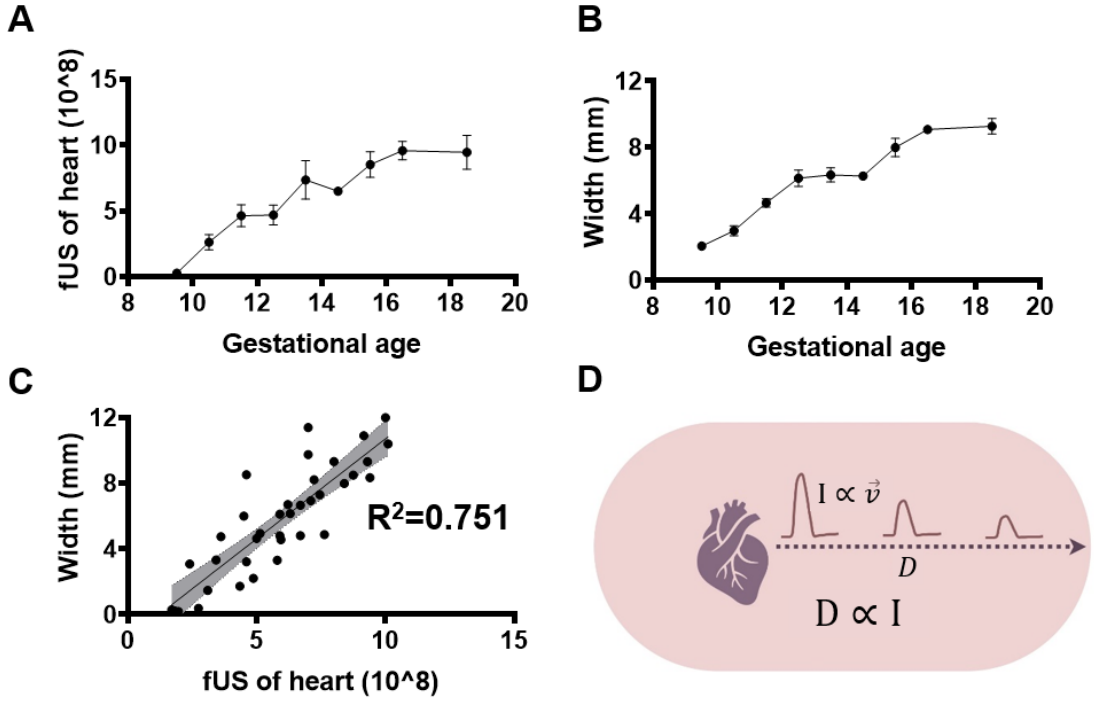

Fig 4: Intensity of Cardiac fUS Signal Couples with Body Size in Embryonic Mice

A) Summary of embryonic cardiac fUS intensity from E9.5 to E18.5, (n=3-6 in each group). Data presented as Mean ± SEM.

B) Summary of embryonic width ranging from E9.5to E18.5, (n=3-6 in each group). Data presented as Mean ± SEM.

C) Correlation analysis of embryonic width versus intensity of cardiac fUS signal during development (R^2=0.703). Data presented as Mean ± SEM.

D) Schematic illustration of the proportional relationship between the observed pattern of blood flow – blood flow from the heart to distal regions – and the corresponding intensity of fUS signals observed.

Abbreviations in Fig. 4: D, distance of heart to distal, i.e. embryonic width; *I*, intensity of cardiac fUS signal; *V*, rate of blood flow.

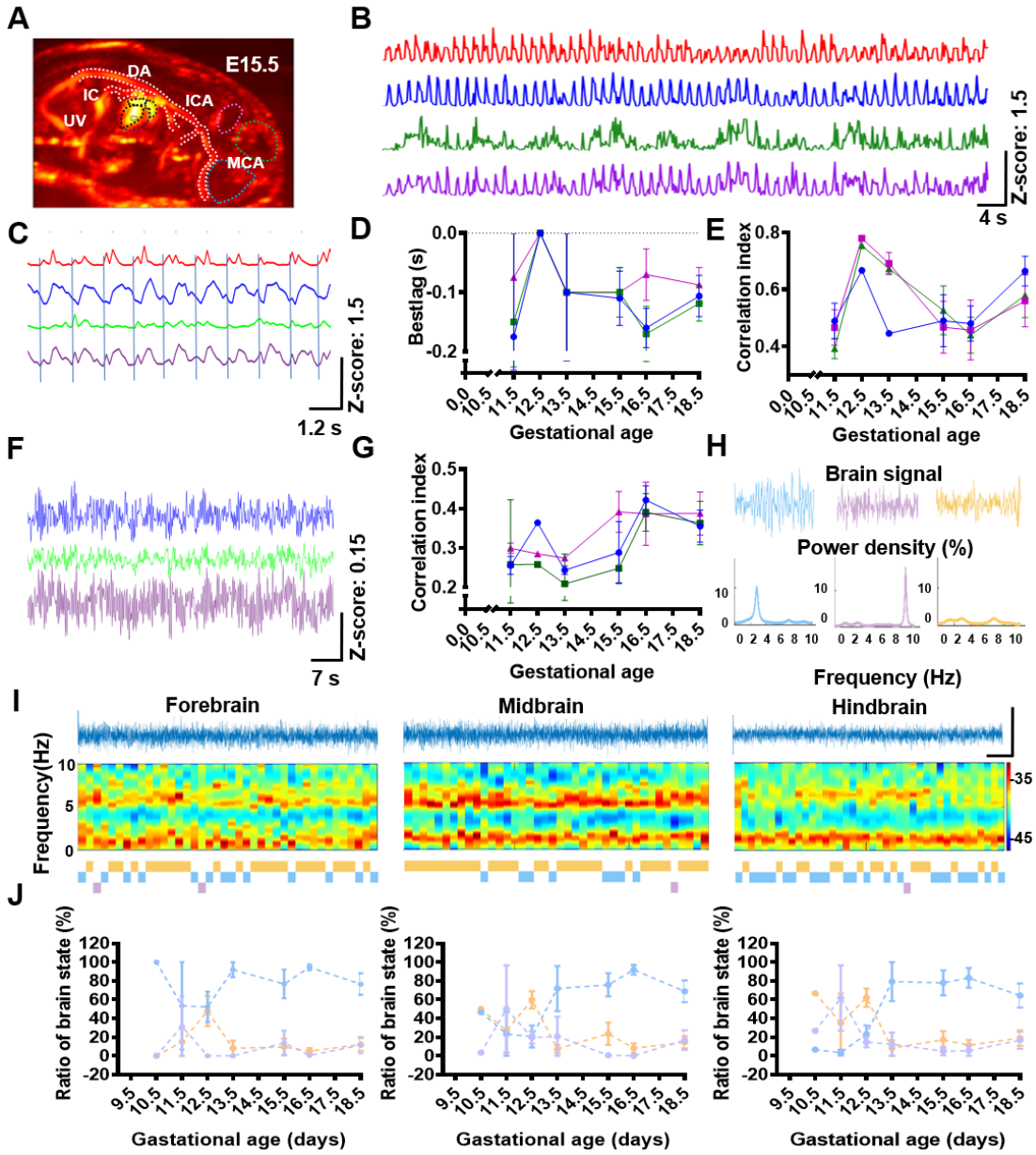

Figure 5: Embryonic brain activity which is independent of the blood flow pulsation is record through functional ultrasound imaging

A) Representative imaging frame of embryonic fUS in an E15.5 mouse (left). Hemodynamic changes were collected from the embryonic heart (black circle), forebrain (blue circle), midbrain (yellow circle), and hindbrain (purple circle).

B) Hemodynamic changes presented as Z-scores. From top to bottom, traces represent heart (red), forebrain (blue), midbrain (green), and hindbrain (purple).

C) Exemplars of fUS signals showing a high correlation between the heart and forebrain, midbrain, and hindbrain (from top to bottom). The brain fUS signals follow the onset of heart activity.

D) Delay in forebrain (blue), midbrain (green), and hindbrain (purple) activity relative to the heart during E11.5 to E18.5 embryonic days (n=2-8 in each group). Data presented as Mean ± SEM.

E) Summarized correlation indices between the heart and forebrain (blue), heart and midbrain (green), and heart and hindbrain (purple), ranging from E11 to E 18.5 (n=2-8 in each group). Data presented as Mean ± SEM.

F) Brain signals in the forebrain (blue), midbrain (green), and hindbrain (purple) (from top to bottom) elucidated after deconvolution analysis.

G) Correlation indices between the three brain regions, i.e., forebrain vs midbrain (blue), midbrain vs hindbrain (green), hindbrain vs forebrain (purple) are summarized ranging from E11.5 to E 18.5 (n=1-8 in each group). Data presented as Mean ± SEM.

H) Principal classification of recorded brain states. Blue signals represent typical slow waves exhibiting a delta rhythm below 4 Hz, purple signals represent typical rapid waves within the theta range of 6 to 10 Hz, and yellow signals represent other epochs with a more even rhythm distribution.

I) Representative signal traces, frequency spectrum and brain state classified every 10 seconds of forebrain, midbrain, and hindbrain (left to right) brain states. Scale bar: 40s & Z-score=05.

J) Summary of forebrain, midbrain, and hindbrain activity (left to right) during the gestational period. Blue: delta rhythm wave; purple: theta wave; yellow: even rhythm. Data presented as Mean ± SEM.

Abbreviations in Fig. 5: DA, dorsal aorta; IC, inferior cava; ICA, internal carotid artery; MCA, middle cerebral artery; UV, umbilical vein.